

Zero-bias anomaly in a nanowire quantum dot coupled to superconductors

Eduardo J. H. Lee¹, Xiaocheng Jiang², Ramon Aguado³, Georgios

Katsaros¹, Charles M. Lieber², and Silvano de Franceschi^{1*}

¹*SPSMS, CEA-INAC/UJF-Grenoble 1, 17 rue des Martyrs, 38054 Grenoble Cedex 9, France*

²*Harvard University, Department of Chemistry and Chemical Biology, Cambridge, MA, 02138, USA and*

³*Instituto de Ciencia de Materiales de Madrid, ICMM-CSIC Cantoblanco, 28049 Madrid, Spain*

(Dated: December 3, 2024)

We studied the low-energy states of spin-1/2 quantum dots defined in InAs/InP nanowires and coupled to aluminium superconducting leads. By varying the superconducting gap, Δ , with a magnetic field, B , we investigated the transition from strong coupling, $\Delta \ll T_K$, to weak coupling, $\Delta \gg T_K$, where T_K is the Kondo temperature. Below the critical field, we observe a persisting zero-bias Kondo resonance that vanishes only for low B or higher temperatures, leaving the room to more robust sub-gap structures at bias voltages between Δ and 2Δ . For strong and approximately symmetric tunnel couplings, a Josephson supercurrent is observed in addition to the Kondo peak. We ascribe the coexistence of a Kondo resonance and a superconducting gap to a significant density of intra-gap quasiparticle states, and the finite-bias sub-gap structures to tunneling through Shiba states. Our results, supported by numerical calculations, own relevance also in relation to tunnel-spectroscopy experiments aiming at the observation of Majorana fermions in hybrid nanostructures.

Hybrid devices which couple superconducting (S) electrical leads to low-dimensional semiconductors have received great attention due to their fascinating underlying physics[1]. Further interest in this field has been generated by recent theoretical predictions on the existence of Majorana fermions at the edges of one-dimensional semiconductor nanowires (NWs) with strong spin-orbit interaction connected to S electrodes [2]. Zero-bias conductance peaks meeting some of the expected characteristic signatures of Majorana physics were recently reported in hybrid devices based on InSb [3, 4] and, more recently, InAs NWs [5]. In the past years, quantum dots (QDs) coupled to superconducting leads have been widely explored as tunable Josephson junctions[6, 7], or as building blocks of Cooper-pair splitters [8, 9], i.e. devices that could serve as sources of entangled pairs of electrons. Hybrid superconductor-QD devices also constitute versatile platforms for studying fundamental issues, such as the physics of the Andreev bound states (ABS) [10, 11] or the interplay between the Kondo effect and the superconducting proximity effect[12–21].

The Kondo effect usually stems from the antiferromagnetic coupling of a localized electron spin and a Fermi sea of conduction electrons. Below a characteristic temperature T_K , the so-called Kondo temperature, a many-body spin-singlet state is formed, leading to the partial or complete screening of the local magnetic moment. This phenomenon, discovered in metals containing diluted magnetic impurities, is now routinely found in individual QDs with a spin-degenerate ground state, e.g. QDs hosting an odd number of electrons. Reasonably high Kondo temperatures (i.e. $T_K > 0.1$ K) can be achieved when the QD is well coupled to normal-type leads. The Kondo effect manifests itself as a zero-bias conductance peak whose width is proportional to T_K . In S -QD- S devices, the quasiparticle density of states (DOS) around the Fermi

level (E_F) of the leads vanishes due to the opening of the superconducting gap (Δ). This lack of quasiparticles precludes Kondo screening.

The competition between the Kondo effect and superconductivity is governed by the corresponding energy scales, $k_B T_K$ and Δ . While no Kondo screening occurs for $k_B T_K \ll \Delta$ (weak coupling), a Kondo singlet is expected to form for $k_B T_K \gg \Delta$ (strong coupling) at the expense of the breaking of Cooper pairs at the Fermi level [15, 22]. A quantum phase transition is predicted to take place at $k_B T_K \approx \Delta$ [12–14]. Experimental signatures of this exotic crossover have been investigated both in the Josephson supercurrent regime [18–20] and in the dissipative sub-gap transport regime [15–17]. Yet a full understanding of these experimental findings is still lacking. In this Letter, we report an experimental study on S -QD- S devices where the relative strength between Kondo and superconducting pairing correlations is tuned by means of a magnetic field, B , acting on the superconducting gap. The transition from strong to weak coupling is continuously accomplished by sweeping B from just above the critical field, B_c , where $\Delta = 0$, to zero field, where Δ attains the maximum value, Δ_0 , exceeding $k_B T_K$.

The S -QD- S devices were fabricated from individual InAs/InP core/shell NWs grown by thermal evaporation (total diameter ~ 30 nm). The InP shell (thickness ~ 2 nm) acts as a confinement barrier resulting in an enhanced mobility of the one-dimensional electron gas in the InAs NW core [23]. After growth, the NWs were deposited onto a degenerately doped, p-type Si substrate (to be used as a back gate), covered by a 300-nm-thick thermal oxide. Device fabrication was accomplished by e-beam lithography, Ar⁺ bombardment (to remove the NW surface oxide), metal evaporation, and lift-off. Source and drain contacts consisted of Ti (2.5 nm)/Al (45 nm) bilayers with a lateral separation of approximately 200 nm, and a superconducting critical temperature of ≈ 1 K. Transport measurements were performed in a He₃-He₄ dilution refrigerator with a base temperature of 15 mK.

* silvano.defranceschi@cea.fr

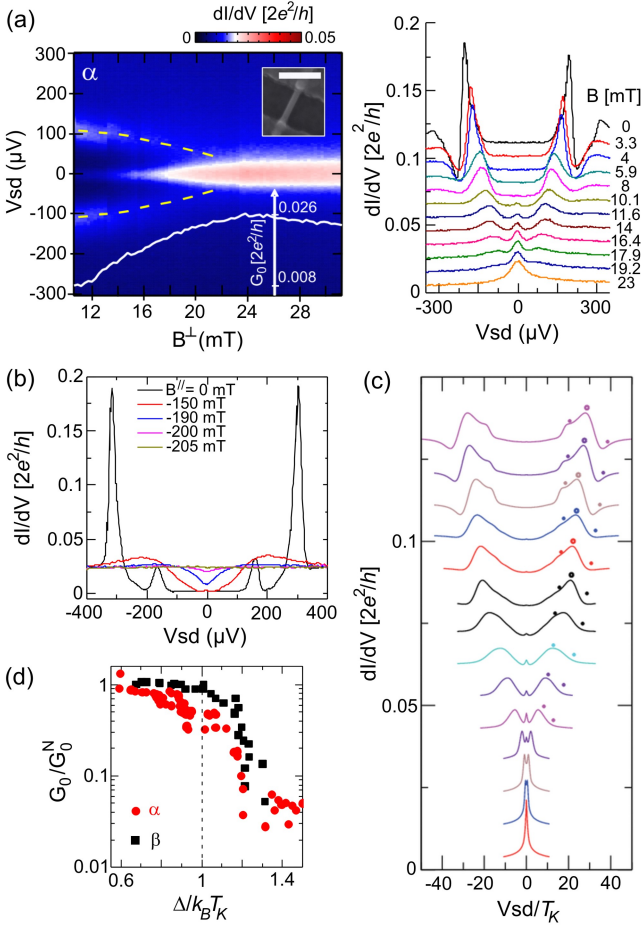


FIG. 1. (color online) (a) Left panel: Color plot of dI/dV vs (B^\perp, V_{sd}) measured at the center of diamond α . The dashed lines highlight the emergence of finite-bias peaks related to the opening of a superconducting gap. The superimposed line trace shows the B^\perp -dependence of the linear conductance. Right panel: $dI/dV(V_{sd})$ traces taken at different B^\perp values. The inset shows a scanning electron micrograph of a typical device (scale bar: 200 nm). (b) $dI/dV(V_{sd})$ traces measured in an even diamond revealing the Dynes-like DOS of the strongly coupled lead. (c) Numerical calculations. The smaller solid dots denote the position of the Δ and 2Δ peaks, whereas the bigger open dots highlight the position of the Shiba bound state peaks. (d) Linear conductance (G_0) normalized to the normal-state value (G_0^N) and plotted as a function of $\Delta/k_B T_K$ for diamonds α (red dots) and β (black squares).

At low temperature, electron transport is dominated by the Coulomb blockade effect with the NW channel behaving as a single QD. Charge stability measurements (i.e. differential conductance, dI/dV , as a function of source-drain bias, V_{sd} , and back-gate voltage, V_G) were performed to identify Kondo resonances in Coulomb diamonds with odd occupation and a spin-1/2 ground state. These measurements were taken at 15 mK with the leads in the normal state (superconductivity was suppressed by means of a magnetic field $B^\perp = 70$ mT perpendicular to the substrate and exceeding the perpendicular

critical field B_c^\perp). In each Kondo diamond, T_K was measured from the half width at half maximum (HWHM) of the zero-bias dI/dV peak, while the tunnel coupling asymmetry was extracted from the peak height, i.e. the linear conductance G , according to the relation: $G/G_0 = 4\Gamma_L\Gamma_R/(\Gamma_L + \Gamma_R)^2$, where $G_0 = 2e^2/h$ and $\Gamma_{L(R)}$ is the tunnel coupling to the left (right) lead. Here we present data corresponding to three Kondo diamonds labeled as α , β and γ , where: $T_{K,\alpha} \approx 0.56$ K, $(\Gamma_L/\Gamma_R)_\alpha \approx 6.6 \times 10^{-3}$, $T_{K,\beta} \approx 1$ K, $(\Gamma_L/\Gamma_R)_\beta \approx 0.44$, and $T_{K,\gamma} \approx 0.71$ K, $(\Gamma_L/\Gamma_R)_\gamma \approx 7.6 \times 10^{-3}$.

Figure 1a shows a $dI/dV(B^\perp, V_{sd})$ measurement taken at the center of Kondo diamond α . The zero-bias Kondo peak is apparent above $B_c^\perp \approx 23$ mT (we note that at such low fields the Zeeman splitting is much smaller than $k_B T_{K,\alpha}$, explaining the absence of a split Kondo peak). Surprisingly, reducing the field below B_c^\perp does not lead to an abrupt suppression of the Kondo peak. Instead, the peak becomes progressively narrower and smaller, vanishing completely only below $B^\perp \approx 9$ mT.

We argue that the observed zero-bias peak is a manifestation of Kondo screening due to intra-gap quasiparticle states. To support this interpretation, we show in Fig. 1b a data set taken in an adjacent diamond with even occupation (i.e. with no Kondo effect). The $dI/dV(V_{sd})$ traces shown correspond to different in-plane fields, B^\parallel , ranging from zero to just above the in-plane critical field $B_c^\parallel \approx 200$ mT. When lowering the fields from above to below B_c^\parallel , the sub-gap dI/dV does not drop abruptly, supporting our hypothesis of a sizable quasiparticle DOS at E_F (we note that, although the measurement of Fig. 1b refers to in-plane fields, a qualitatively similar behavior can be expected for perpendicular fields). The development of a "soft" gap just below the critical field is additionally marked by the absence of dI/dV peaks characteristic of the BCS DOS singularities. Such peaks develop only at fields well below B_c^\parallel , becoming most pronounced at $B = 0$. In this low-field limit, the sub-gap conductance simultaneously vanishes and first-order multiple-Andreev-reflection resonances emerge at $eV_{sd} \approx \pm\Delta$.

To reproduce the observed sub-gap features and the coexistence of a Kondo peak and a superconducting gap, we calculated the dI/dV of a QD modeled by an Anderson Hamiltonian including coupling to BCS-type superconducting reservoirs. We used the so-called non-crossing approximation, a fully non-perturbative theory that includes both thermal and quantum fluctuations, complemented with the Keldysh-Green's function method to take into account non-equilibrium effects at finite V_{sd} (see Supplemental Material). In order to fit the experimental data, the DOS of the leads was modeled by a Dynes function:

$$N_s(E, \gamma, B) = \text{Re} \left[\frac{|E| + i\gamma(B)}{\sqrt{(|E| + i\gamma(B))^2 - \Delta(B)^2}} \right], \quad (1)$$

where $\gamma(B)$ is a phenomenological broadening term. For small $\Delta(B)$, the $\gamma(B)$ term is particularly important leading to a finite quasiparticle DOS at E_F . By contrast, as $\Delta(B)$ increases (with decreasing B), the DOS

of the superconducting leads approaches the ideal (i.e. unbroadened) BCS profile.

Figure 1c shows a set of calculated $dI/dV(V_{sd})$ traces at different magnetic fields. By adjusting the DOS parameters $\gamma(B)$ and $\Delta(B)$, these calculations clearly show a zero-bias peak persisting below the critical field, in agreement with the experimental data of Fig. 1a. Since this peak emerges only in the case of a finite $\gamma(B)$, we conclude that the finite DOS at the Fermi level is at the origin of the experimentally observed zero-bias anomaly. The narrowing of this Kondo anomaly with increasing Δ can be interpreted as a decreasing T_K due to the shrinking quasiparticle DOS around the Fermi level (this aspect is more quantitatively discussed further below). As T_K approaches the electronic temperature also the peak height gets smaller leading to the disappearance of the zero-bias peak.

Figure 2 shows a second data set taken in Kondo diamond β . In this case, the stronger and more symmetric coupling to the leads results in a higher T_K , and a larger peak conductance. Nevertheless, the field dependence (Fig. 2a) shows substantially the same behavior as in Fig. 1a, i.e. a zero-bias Kondo peak persisting below B_c^\perp , becoming progressively narrower with decreasing B^\perp , and vanishing below $B^\perp \approx 10$ mT. Interestingly, a sharp dI/dV resonance is found around $V_{sd} = 0$ superimposed to the (wider) zero-bias Kondo peak. This resonance persists throughout the entire field range in which the leads are superconducting (see Figs. 2a and 2b). By performing current-bias measurements (inset of Fig. 2b), we were able to ascribe this sharp resonance to a dissipationless Josephson supercurrent as high as 0.9 nA at $B = 0$. This finding reveals the possibility of a coexistence between the Josephson effect, linked to the superconducting nature of the leads, and a Kondo effect arising from the exchange coupling between the localized electron and intra-gap quasiparticle states.

Temperature dependence measurements performed in diamond β (Figs. 2c and 2d, see also Supplemental Material) show that in the regime of coexistence between the Kondo effect and superconductivity, the height of the persisting Kondo anomaly follows the usual T -dependence for a normal state regime given by $G(T)/G_0 = [1/(1 + (T/T_K^*)^2)]^s$, where $T_K^* = T_K^*/\sqrt{2^{1/s} - 1}$, $s = 0.22$ and T_K^* is the effective Kondo temperature [24]. In addition, we show that T_K^* decreases with decreasing B^\perp (inset of Fig. 2d), as expected from the reduced intra-gap quasiparticle DOS.

At base temperature, the peak heights of Kondo resonances α and β appear to follow approximately the same dependence on $\Delta/k_B T_K$ (Fig. 1d), where T_K refers to the Kondo temperature in the normal state. A similar scaling was reported earlier by Buizert et al. [15], for a S-QD-S device fabricated from an InAs self-assembled quantum dot using Ti/Al contacts. In that paper, it was speculated that when $k_B T_K \gg \Delta$, it becomes energetically favorable for Cooper pairs to split in order to screen the local spin and create a Kondo resonance at the Fermi level. The results presented here point at a differ-

ent interpretation based on the presence of the already discussed intra-gap quasiparticle states, which become particularly important when B approaches B_c . According to this interpretation, the apparent scaling in Fig. 1d is intimately related to a quasi-particle "poisoning" of the superconducting gap.

Well below the critical field, as the zero-bias Kondo anomaly disappears, the $dI/dV(V_{sd})$ is dominated by a pair of peaks symmetrically positioned with respect to $V_{sd} = 0$ (Fig. 1a). These peaks become most pronounced at $B = 0$. Similar types of sub-gap structures have been reported in earlier works and they were given different interpretations: a Kondo enhancement of the first order multiple Andreev reflection process [15, 17], or, in the case of asymmetrically coupled S-QD-S devices, a persisting Kondo resonance, created by the strongly coupled lead, which is probed by the BCS DOS of the second, weakly-coupled lead [16]. Both of the above interpretations invoke Kondo correlations to explain the observed sub-gap structure, even though, as we have pointed out, these correlations get suppressed as the superconducting gap reaches its largest value at $B = 0$. More recently, it was shown that the finite-bias sub-gap structure can be explained in terms of tunneling through magnetic Andreev bound states [25, 26].

The problem of a magnetic impurity interacting with a superconductor was addressed already in the sixties by Yu, Shiba and Rusinov [27]. It was shown that intra-gap Andreev bound states, now often called Shiba states, emerge as a result of the exchange coupling, J , between the impurity and the superconductor. As later confirmed by experiments based on scanning tunneling spectroscopy [28], Shiba states emerge as pairs of peaks in the local DOS symmetrically positioned at energies $\pm E_B$ relative to the Fermi level, where E_B depends on J and $|E_B| < \Delta$.

The zero-field $dI/dV(V_{sd})$ trace in the right panel of Fig. 1a exhibits a pair of dI/dV peaks at $eV_{sd} \approx \pm 1.4\Delta$, followed by negative dI/dV regions. Taking into account the strong asymmetry in the tunnel couplings, these features can be well explained in terms of a pair of Shiba levels with $E_B = 0.4\Delta$, created by the strongly coupled S lead, and tunnel-probed by the weakly coupled S lead (see Fig. 3a). The observed dI/dV peaks result from the alignment of these Shiba levels with the BCS gap-edge singularities. Precisely, one dI/dV peak is due to the onset of electron tunneling from the Shiba level below E_F to the empty quasi-particle band of the S probe. The other peak is due to the onset of electron tunneling from the occupied quasi-particle band of the S probe to the Shiba level above E_F . Increasing $|V_{sd}|$ beyond these resonance conditions leads to a reduced tunneling probability and hence a negative dI/dV . The Shiba-related features observed in Fig. 1a are very well reproduced by the numerical results in Fig. 1c. A significantly different sub-gap structure is found in the case of relatively low contact asymmetry, as clearly shown in the lower panel of Fig. 2b. Here, both S leads interact with the QD spin resulting in a stronger exchange coupling. We find a pair of dI/dV peaks at $eV_{sd} \approx \pm \Delta$, which implies $E_B \approx 0$.

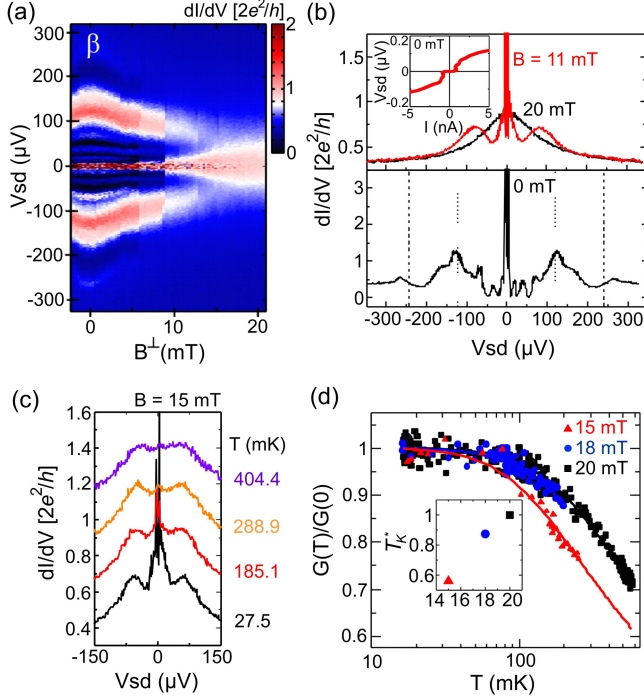


FIG. 2. (color online) (a) Out-of-plane field dependence measured in diamond β . (b) dI/dV line profiles taken at different magnetic fields. The inset is a voltage-current measurement carried out at $B = 0$, which reveal transport of a dissipationless supercurrent in the device. (c) Evolution of the dI/dV measured at $B^\perp \approx 15$ mT, as a function of the temperature (T). The zero-bias Kondo peak and the gap-related side peaks show distinct T dependences. The former is strongly suppressed with increasing T . (d) Temperature dependence of the normalized conductance of the zero-bias Kondo peak measured either above (squares) or below (circles and triangles) B_c^\perp . $G(0)$ denotes the peak height measured at base temperature. The inset reveals that the effective Kondo temperature T_K^* decreases with increasing Δ .

In addition, we observe a rather complex set of smaller peaks most likely due to multiple Andreev reflection processes.

In the weak-coupling limit, the energy of the Shiba states is related to the superconducting gap through $E_B = \Delta(1-x)/(1+x)$, where $x = 3(\pi\nu_F J/4)^2$ and ν_F is the Fermi velocity [26]. Since J is presumably independent of B , the energy of the Shiba states should evolve proportionally to $\Delta(B)$ as B is varied. We have verified this dependence with a measurement performed in diamond γ , where, as in diamond α , tunnel couplings are strongly asymmetric. Differently from diamond α , however, the low-energy transport is characterized by two pairs of intra-gap dI/dV peaks, as shown by the zero-field curve in Fig. 3c. As in Fig. 1a, the most prominent peaks (at $eV_{sd} \sim \pm 1.4\Delta$) correspond to the alignment of the Shiba levels with the BCS coherence peaks of the weakly coupled contact, and they are consistently followed by negative dI/dV dips. The weaker peaks at $eV_{sd} \approx \pm 0.55\Delta$ (in fact only one of them is clearly vis-

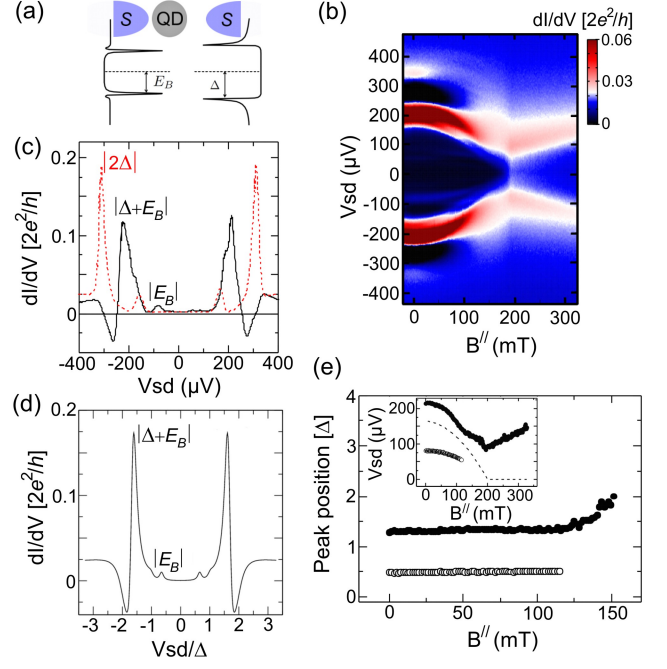


FIG. 3. (color online) (a) Schematics of the formation of YSR bound states resulting from the interaction of the QD with the strongly-coupled lead. (b) Differential conductance measured in diamond γ as a function of the in-plane magnetic field. (c) The solid line depicts the dI/dV taken at $B = 0$. Two pairs of peaks are observed at $|eV_{sd}| = \Delta + E_B, E_B$. The dashed line shows the equivalent dI/dV taken in an even diamond, for comparison. (d) Numerical calculation of the dI/dV for $B = 0$. (e) Position of the intra-gap peaks as a function of the magnetic field. The inset shows the data before performing the rescaling in units of Δ . The dashed line displays the field-dependence of Δ .

ible) can be interpreted as 'replicas' of the Shiba peaks. Such 'replicas' are expected when the Shiba levels line up with the Fermi level of the weakly coupled S lead (for $eV_{sd} = \pm E_B$), provided a non negligible density of quasi-particles is present throughout its superconducting gap. This is apparent from the calculated $dI/dV(V_{sd})$ trace in Fig. 3d, which agrees fairly well with the experimental one.

The Shiba peaks and their replicas shift towards $V_{sd} = 0$ as B^\parallel is increased. Their voltage positions are plotted in the inset of Fig. 3e as solid and open dots, respectively. For comparison, the $\Delta(B^\parallel)$ dependence measured in a non-Kondo diamond (with even electron number) is also plotted in the same inset (dashed line). Up to $B^\parallel \sim 120$ mT, the Shiba peaks and their replicas evolve proportionally to $\Delta(B^\parallel)$ in agreement with the theoretical prediction. Above $B^\parallel \sim 120$ mT, this behavior begins to be affected by the increasing Zeeman splitting (≈ 0.3 eV/T) of the QD spin doublet. The main Shiba peaks get strongly suppressed and they seem to eventually merge into the normal-state, Zeeman-split Kondo peaks through a non-trivial transition region (roughly between 120 and 180 mT). In this parallel-field configura-

tion, the large Zeeman splitting at $B^{\parallel} \approx B_c^{\parallel}$ prevents the observation of a zero-bias Kondo peak when approaching B_c^{\parallel} .

In conclusion, we have studied the transport properties of a spin-1/2 QD coupled to S contacts. The ability to continuously tune the superconducting gap with an external magnetic field enabled us to investigate the transition from a normal-state Kondo to a superconducting-state Shiba ground state. We showed that the presence of a finite quasiparticle DOS within the superconducting gap can promote the formation of a zero-bias Kondo peak coexisting with superconductivity. The origin of this quasiparticle DOS remains to be clarified, also through a better understanding of the superconducting proximity effect in semiconductor nanowire structures (e.g., the role of disorder-induced pair breaking [29]). Finally, we should like to emphasize that our results bear clear impli-

cations in the interpretation of sub-gap transport features in hybrid superconductor-semiconductor systems, especially in the presence of relatively high magnetic fields that can cause a significant suppression of the superconducting gap. This is precisely the regime where Majorana fermions are expected to arise as zero-energy quasiparticle states. We argue that intra-gap quasiparticle states, manifesting through a sizable background conductance (which is the case of experiments reported in Refs. 3–5), could result in the screening of a local spin (or orbital) degeneracy leading to zero-bias anomalies that are not related to Majorana physics.

This work was supported by the EU Marie Curie program and by the Agence Nationale de la Recherche. R. A. acknowledges support from the Spanish Ministry of Science and Innovation through grant FIS2009-08744.

-
- [1] S. D. Franceschi, L. P. Kouwenhoven, C. Schonenberger, and W. Wernsdorfer, *Nature Nanotech.* **5**, 703 (2010).
 - [2] R. M. Lutchyn, J. D. Sau, and S. D. Sarma, *Phys. Rev. Lett.* **105**, 077001 (2010).
 - [3] V. Mourik, K. Zuo, S. M. Frolov, S. R. Plissard, E. P. A. M. Bakkers, and L. P. Kouwenhoven, *Science* **336**, 1003 (2012).
 - [4] M. T. Deng, C. L. Yu, G. Y. Huang, M. Larsson, P. Caroff, and H. Q. Xu, *arXiv:1204.4130v1* (2012).
 - [5] A. Das, Y. Ronen, Y. Most, Y. Oreg, M. Heiblum, and H. Shtrikman, *arXiv:1205.7073v1* (2012).
 - [6] J. A. van Dam, Y. V. Nazarov, E. P. A. M. Bakkers, S. D. Franceschi, and L. P. Kouwenhoven, *Nature* **442**, 667 (2006).
 - [7] J. Cleuziou, W. Wernsdorfer, V. Bouchiat, T. Ondarcuhu, and M. Monthieux, *Nature Nanotech.* **1**, 53 (2006).
 - [8] L. Hofstetter, S. Csonka, J. Nygard, and C. Schonenberger, *Nature* **461**, 960 (2009).
 - [9] L. G. Herrmann, F. Portier, P. Roche, A. L. Yeyati, T. Kontos, and C. Strunk, *Phys. Rev. Lett.* **104**, 026801 (2010).
 - [10] J. D. Pillet, C. H. L. Quay, P. Morfin, C. B. abd A. Levy Yeyati, and P. Joyez, *Nature Phys.* **6**, 965 (2010).
 - [11] R. S. Deacon, Y. Tanaka, A. Oiwa, R. Sakano, K. Yoshida, K. Shibata, K. Hirakawa, and S. Tarucha, *Phys. Rev. Lett.* **104**, 076805 (2010).
 - [12] F. Siano and R. Egger, *Phys. Rev. Lett.* **93**, 047002 (2004).
 - [13] M. S. Choi, M. Lee, K. Kang, and W. Belzig, *Phys. Rev. B* **70**, 020502(R) (2004).
 - [14] A. Oguri, Y. Tanaka, and A. C. Hewson, *J. Phys. Soc. Japan* **73**, 2494 (2004).
 - [15] C. Buizert, A. Oiwa, K. Shibata, K. Hirakawa, and S. Tarucha, *Phys. Rev. Lett.* **99**, 136806 (2007).
 - [16] A. Eichler, M. Weiss, S. Oberholzer, C. Schonenberger, A. L. Yeyati, J. C. Cuevas, and A. Martin-Rodero, *Phys. Rev. Lett.* **99**, 126602 (2007).
 - [17] T. Sand-Jespersen, J. Paaske, B. M. Andersen, K. Grove-Rasmussen, H. I. Jorgensen, M. Aagesen, C. B. Sorensen, P. E. Lindelof, K. Flensberg, and J. Nygard, *Phys. Rev. Lett.* **99**, 126603 (2007).
 - [18] Y. Kanai, R. S. Deacon, O. Oiwa, K. Yoshida, K. Shibata, K. Hirakawa, and S. Tarucha, *Phys. Rev. Lett.* **2010**, 054512 (2010).
 - [19] K. Grove-Rasmussen, H. Jorgensen, and P. Lindelof, *New J. Phys.* **9**, 124 (2007).
 - [20] A. Eichler, R. Deblock, M. Weiss, C. Karrasch, V. Meden, and C. Schonenberger, *Phys. Rev. B* **79**, 161407 (2009).
 - [21] K. J. Franke, G. Schulze, and J. I. Pascual, *Science* **332**, 940 (2011).
 - [22] L. I. Glazman and K. Matveev, *JETP Lett.* **49**, 659 (1989).
 - [23] X. Jiang, Q. Xiong, F. Qian, Y. Li, and C. M. Lieber, *Nano Lett.* **7**, 3214 (2007).
 - [24] D. Goldhaber-Gordon, J. Gores, M. A. Kastner, H. Shtrikman, D. Mahalu, and U. Meirav, *Phys. Rev. Lett.* **81**, 5225 (1998).
 - [25] V. Koerting, B. M. Andersen, K. Flensberg, and J. Paaske, *Phys. Rev. B* **2010**, 245108 (2010).
 - [26] B. M. Andersen, K. Flensberg, V. Koerting, and J. Paaske, *Phys. Rev. Lett.* **107**, 256802 (2011).
 - [27] A. V. Balatsky, I. Vekhter, and J. X. Zhu, *Rev. Mod. Phys.* **78**, 373 (2006).
 - [28] A. Yazdani, B. A. Jones, C. P. Lutz, M. F. Crommie, and D. M. Eigler, *Science* **275**, 1767 (1997).
 - [29] J. Liu, A. C. Potter, K. T. Law, and P. A. Lee, *arXiv:1206.1276v1* (2012).

Supplemental Material: Zero-bias anomaly in a nanowire quantum dot coupled to superconductors

Eduardo J. H. Lee¹, Xiaocheng Jiang², Ramon Aguado³, Georgios

Katsaros¹, Charles M. Lieber², and Silvano de Franceschi^{1*}

¹*SPSMS, CEA-INAC/UJF-Grenoble 1, 17 rue des Martyrs, 38054 Grenoble Cedex 9, France*

²*Harvard University, Department of Chemistry and Chemical Biology, Cambridge, MA, 02138, USA and*

³*Instituto de Ciencia de Materiales de Madrid, ICMM-CSIC Cantoblanco, 28049 Madrid, Spain*

Model

The dot is described by an Anderson Hamiltonian

$$H_D = \sum_{\sigma=\uparrow,\downarrow} \varepsilon_\sigma d_\sigma^\dagger d_\sigma + U n_\uparrow n_\downarrow, \quad (1)$$

where ε_σ is the single-particle energy level of the localized state with spin σ , d_σ^\dagger (d_σ) the fermion creation (annihilation) operator of the state, $n_\sigma = d_\sigma^\dagger d_\sigma$ the occupation, and U the on-site Coulomb interaction, which defines the charging energy. We focus on a regime where the charging energy is much bigger than other energy scales. In this regime the Hamiltonian in Eq. (1) suffices to describe all relevant physics.

Kondo physics arises as a result of the interplay between the strong correlation in the dot and the coupling of the localized electrons with the electrons in conduction bands. In our case, these are described as two leads ($\alpha = L$ and R) which can be either normal or superconducting. In this later case, they are represented by a BCS hamiltonian of the form:

$$H_\alpha = \sum_{k_\alpha} \sum_{\sigma} \varepsilon_{k_\alpha, \sigma} a_{k_\alpha \sigma}^\dagger a_{k_\alpha \sigma} + \sum_{k_\alpha} \Delta (a_{k_\alpha \uparrow}^\dagger a_{-k_\alpha \downarrow}^\dagger + h.c.) \quad (2)$$

with Δ being the superconducting pairing gap. Tunneling is described by the Hamiltonian

$$H_T = \sum_{k_\alpha \sigma} \left(V_{k_\alpha \sigma} a_{k_\alpha \sigma}^\dagger d_\sigma + h.c. \right). \quad (3)$$

The total Hamiltonian is then given by $H = H_L + H_R + H_T + H_D$. For simplicity, we ignore the k - and σ -dependence of the tunneling amplitudes. Therefore, we consider a simplified model with $V_{k_\alpha \sigma} = V_\alpha / \sqrt{2}$ which defines the widths $\Gamma_\alpha^N = \pi \rho_0 |V_\alpha|^2$, where ρ_0 is the (normal) density of states in the reservoirs. In the presence of superconductivity, the coupling to the reservoirs is modified due to the BCS density of states as

$$\Gamma_\alpha(E) = \Gamma_\alpha^N N_s(E, B) = \Gamma_\alpha^N \text{Re} \frac{|E|}{\sqrt{|E|^2 - \Delta(B)^2}}. \quad (4)$$

This, of course, corresponds to a clean BCS case. As discussed in the main text, it is clear from the experimental data in even diamonds that the clean BCS case is not a good description of the experiments. Instead, a Dynes expression of the form

$$N_s(E, \gamma, B) = \text{Re} \left[\frac{|E| + i\gamma(B)}{\sqrt{(|E| + i\gamma(B))^2 - \Delta(B)^2}} \right], \quad (5)$$

has to be used, where $\gamma(B)$ is a phenomenological broadening which takes into account a finite density of states inside the BCS gap.

Non-crossing approximation method

Now we write the physical fermionic operator as a combination of a pseudofermion and a boson operator as follows: $d_\sigma = b^\dagger f_\sigma$ where f_σ is the pseudofermion which annihilates one "occupied state" with spin σ , and b^\dagger is a boson

operator which creates an "empty state". We are interested in a limit where the Coulomb interaction is very large such that we can safely take the limit of $U \rightarrow \infty$. This fact enforces the constraint $\sum_{\sigma} f_{\sigma}^{\dagger} f_{\sigma} + b^{\dagger} b = 1$, that prevents the accommodation of two electrons at the same time in QD level. This constraint is treated with a Lagrange multiplier.

$$H_{\text{SB}} = \sum_{k_L, \sigma} \varepsilon_{k_L, \sigma} a_{k_L, \sigma}^{\dagger} a_{k_L, \sigma} + \sum_{k_L} \Delta (a_{k_L, \uparrow}^{\dagger} a_{-k_L, \downarrow}^{\dagger} + h.c.) + \sum_{\sigma} \varepsilon_{\sigma} f_{\sigma}^{\dagger} f_{\sigma} + \frac{\bar{V}_L}{\sqrt{N}} \sum_{k_L, \sigma} (c_{k_L, \sigma}^{\dagger} b^{\dagger} f_{\sigma} + h.c.) + (L \rightarrow R) + \lambda \left(\sum_{\sigma} f_{\sigma}^{\dagger} f_{\sigma} + b^{\dagger} b - 1 \right). \quad (6)$$

Notice that we have rescaled the tunneling amplitudes $V_{\alpha} \rightarrow \bar{V}_{\alpha} \sqrt{N}$ according to the spirit of a $1/N$ -expansion (N is the total degeneracy of the localized orbital).

Our next task is to solve this Hamiltonian, which is rather complicated due to the presence of the three operators in the tunneling part and the constrain. Moreover, we need to take into account superconductivity and non-equilibrium effects. In order to do this we employ the so-called Non-Crossing approximation (NCA) [1–4] generalized to the superconducting case [5, 6]. Without entering into much detail of the theory, we just mention that the boson fields in Eq. (6) are treated as fluctuating operators such that both thermal and charge fluctuations are included in a self-consistent manner. In particular, one has to derive self-consistent equations-of-motion for the time-ordered double-time Green's function (sub-indexes are omitted here):

$$\begin{aligned} iG(t, t') &\equiv \langle T_c f(t) f^{\dagger}(t') \rangle, \\ iB(t, t') &\equiv \langle T_c b(t) b^{\dagger}(t') \rangle, \end{aligned} \quad (7)$$

or in terms of their analytic pieces:

$$\begin{aligned} iG(t, t') &= G^{>}(t, t') \theta(t - t') - G^{<}(t, t') \theta(t' - t), \\ iB(t, t') &= B^{>}(t, t') \theta(t - t') + B^{<}(t, t') \theta(t' - t); \end{aligned} \quad (8)$$

A rigorous and well established way to derive these equations-of-motion was first introduced by Kadanoff and Baym [7], and has been related to other non-equilibrium methods (like the Keldysh method) by Langreth, see Ref. [8] for a review. In the paper, we just show numerical results of the coupled set of integral NCA equations for our problem and refer the interested reader to Refs. [1–4] for details. In particular, the density of states is given by

$$\rho(\omega) = -\frac{1}{\pi} \sum_{\sigma} \text{Im}[A_{\sigma}^r(\omega)], \quad (9)$$

where $A_{\sigma}^r(\varepsilon)$ is the Fourier transform of the retarded Green's function $A_{\sigma}^r(t) = G_{\sigma}^r(t) B^{<}(-t) - G_{\sigma}^{<}(t) B^a(-t)$. Note that this decoupling neglects vertex corrections and, as a result, the NCA fails in describing the low-energy Fermi-liquid regime. Nevertheless, the NCA has proven to give reliable results even at temperatures well below the Kondo temperature (of the order of $T = 10^{-2} T_K$) [9]. Following Meir and Wingreen in Ref. [10], the current is given by:

$$I_{\alpha \in \{L, R\}} = -\frac{2e}{h} \sum_{\sigma} \int d\epsilon \Gamma_{\alpha}(\epsilon) [2 \text{Im} A_{\sigma}^r(\epsilon) f_{\alpha}(\epsilon) + A_{\sigma}^{<}(\epsilon)]. \quad (10)$$

with $A_{\sigma}^{<}(\epsilon)$ the Fourier transform of $A_{\sigma}^{<}(t) = iG_{\sigma}^{<}(t) [B^r(-t) - B^a(-t)]$ and $f_{\alpha}(\epsilon) = \frac{1}{1 + e^{\frac{(\epsilon - \mu_{\alpha})}{kT}}}$ the Fermi-Dirac function at each reservoir held at a chemical potential μ_{α} such that the applied bias voltage is defined as $eV = \mu_R - \mu_L$.

In practice, we selfconsistently solve the NCA integral equations until good numerical convergence is reached. All dI/dV calculations presented in the main text are done for finite temperatures $T = 0.25 T_K$ and increasing values of Δ , roughly from $\Delta = 0$ (bottom curve of Fig. 1c) to $\Delta = 20 T_K$ (top curve of Fig. 1c).

"Soft" gaps in out-of-plane and in-plane magnetic fields

Here we present measurements in which the magnetic field dependence of the superconducting gap Δ was probed both in out-of-plane and in-plane configurations. For this purpose, we have performed measurements using S-QD-N devices, which are identical to the devices discussed in the main text, except for the fact that one of the S aluminium

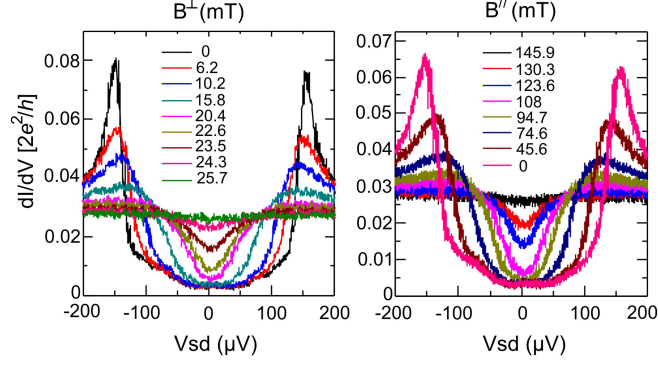


FIG. 1: Magnetic field dependence of the superconducting gap measured in an out-of-plane (left panel) or in an in-plane (right panel) configuration.

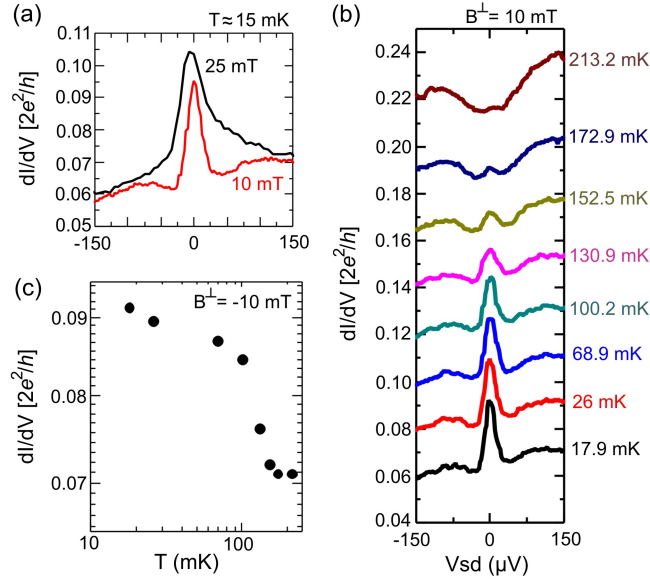


FIG. 2: (a) Persistence and narrowing of the Kondo peak below B_c . The side peaks observed in the red trace are related to the superconducting gap (see main text). (b) Temperature dependence of the persisting zero-bias Kondo anomaly. (c) dI/dV of the zero-bias peak plotted as a function of the temperature.

leads is replaced by a normal metal Au contact. The data shown in Fig. 1 was taken in an even valley, i.e. in the absence of Kondo correlations. In agreement with our discussion in the main text, the transition from the normal to the superconducting regimes is characterized by the opening of a "soft" gap, which is populated by intra-gap quasiparticle states. As B decreases, the intra-gap DOS decreases, until a well-defined gap is obtained for low fields. The out-of-plane and in-plane field dependences are qualitatively identical, except for the different critical fields.

Temperature dependence of a different Kondo resonance

Here we present data corresponding to the temperature (T) dependence of a different Kondo resonance δ ($T_{K,\delta} \approx 0.35$ K). First, we verified that the overall magnetic field behavior of δ is qualitatively identical to that observed in diamonds α , β and γ , as described in the main text. Fig. 2a depicts the persistence and narrowing of the zero-bias Kondo peak below the critical field B_c^{\perp} . Side peaks related to the superconducting gap are also visible. The temperature dependence measurements were taken at $B^{\perp} = 10$ mT. Fig. 2b clearly shows the distinct temperature dependences of the zero-bias peak and the side peaks. Indeed the zero-bias peak is strongly suppressed whereas the

side peaks are only weakly affected. This relates to the fact that the zero-bias peak follows a Kondo temperature dependence, which is expected to yield a 40% drop in conductance for $T = 0.2$ K and $T_{K,\delta} \approx 0.35$ K. The discrepancy in comparison with the experimental data (shown in Fig. 2c) most likely arises due to the intra-gap quasiparticle DOS (see main text), which gives rise to a finite dI/dV at zero-bias even when the Kondo peak is thermally suppressed. On the other hand, the superconducting gap at $B = 0$, $\Delta_0 \approx 150$ μeV , is only reduced in $\approx 10\%$ at $T = 0.2$ K. Therefore, the position of the side peaks observed in Fig. 2b are only marginally affected by T .

* Electronic address: silvano.defranceschi@cea.fr

- [1] David C. Langreth and Peter Nordlander, Phys. Rev. B, **43**, 2541 (1991).
- [2] Ned S. Wingreen and Yigal Meir, Phys. Rev. B, **49**, 11040 (1994)
- [3] Matthias H. Hettler, Johann Kroha and Selman Hershfield, Phys. Rev. Lett., **73**, 1967 (1994); Phys. Rev. B, **58**, 5649 (1998).
- [4] R. Aguado and D.C. Langreth, Phys. Rev. B **67**, 245307 (2003).
- [5] A. A. Clerk and V. Ambegaokar, Phys. Rev. B **61**, 9109 (2000).
- [6] Gabriel Sellier, Thilo Kopp, Johann Kroha, and Yuri S. Barash Phys. Rev. B **72**, 174502 (2005)
- [7] L. P. Kadanoff and G. Baym, *Quantum Statistical Mechanics* (Benjamin, New York, 1962).
- [8] D.C. Langreth, in *Linear and Nonlinear Electron Transport in Solids, Nato ASI, Series B* vol. 17, edited by J.T. Devreese and V.E. Van Doren (Plenum, New York, 1976).
- [9] T.A. Costi, J. Kroha, and P. Wlfle, Phys. Rev. B **53**, 1850 (1996)
- [10] Y. Meir and N. S. Wingreen, Phys. Rev. Lett. **68**, 2512 (1992).